OpenACC GPU implementation of double-stage delay-multiply-and-sum algorithm
Toward enhanced real-time linear-array photoacoustic tomography

Miri Rostami, Seyyed Reza; Mozaffarzadeh, Moein; Hariri, Ali; Jokerst, Jesse V.; Ghaffari-Miab, Mohsen

DOI
10.1117/12.2511115

Publication date
2019

Document Version
Final published version

Published in
Proceedings of SPIE

PROCEEDINGS OF SPIE

SPIEDigitalLibrary.org/conference-proceedings-of-spie

OpenACC GPU implementation of double-stage delay-multiply-and-sum algorithm: toward enhanced real-time linear-array photoacoustic tomography

Miri Rostami, Seyyed Reza, Mozaffarzadeh, Moein, Hariri, Ali, Jokerst, Jesse, Ghaffari-Miab, Mohsen

Seyyed Reza Miri Rostami, Moein Mozaffarzadeh, Ali Hariri, Jesse V. Jokerst, Mohsen Ghaffari-Miab, "OpenACC GPU implementation of double-stage delay-multiply-and-sum algorithm: toward enhanced real-time linear-array photoacoustic tomography," Proc. SPIE 10878, Photons Plus Ultrasound: Imaging and Sensing 2019, 108785C (27 February 2019); doi: 10.1117/12.2511115

SPIE.

Event: SPIE BiOS, 2019, San Francisco, California, United States

OpenACC GPU Implementation of Double-Stage Delay-Multiply-and-Sum Algorithm: Toward Enhanced Real-Time Linear-Array Photoacoustic Tomography

Seyyed Reza Miri Rostami[a], Moein Mozaffarzadeh[a,b], Ali Hariri[c], Jesse Jokerst[c,d,e], and Mohsen Ghaffari-Miab[a]

[a]Computational Electromagnetics Laboratory, Department of Electrical and Computer Engineering, Tarbiat Modares University, Tehran, Iran
[b]Laboratory of Acoustical Wavefield Imaging, Department of Imaging Physics, Delft University of Technology, Delft, The Netherlands
[c]Department of NanoEngineering, University of California, San Diego, 9500 Gilman Drive, La Jolla, CA 92092, United States
[d]Materials Science and Engineering Program, University of California, San Diego, 9500Gilman Drive, La Jolla, CA 92092, United States
[e]Department of Radiology, University of California, San Diego, 9500 Gilman Drive, La Jolla, CA 92092, United States

ABSTRACT

double-stage delay-multiply-and-sum (DS-DMAS) is one of the algorithms proposed for photoacoustic image reconstruction where a linear-array transducer is used to detect signals. This algorithm provides a higher contrast image in comparison with the conventional delay-multiply-and-sum (DMAS) and delay-and-sum (DAS), but it imposes a high computational complexity. In this paper, open accelerators (OpenACC) GPU computation parallel approach is used to lessen the computational time and address the high computational time of the DS-DMAS for photoacoustic image reconstruction process. Compared with sequential execution of the DS-DMAS on CPU, a speed-up of approximately 74× is achieved (for an image having 1024 × 1024 pixels). The proposed approach provides possibility to have an accurate reconstructed photoacoustic image with a reasonable frame rate. In addition, the higher the number of the image pixels, the higher speed-up is achieved. Using the suggested GPU implementation, it is feasible to reconstruct photoacoustic images having a size of 128 × 128, and 256 × 256 with a frame rate of 3 and 2, respectively.

Keywords: Graphics Processing Unit (GPU), Central Processing Unit (CPU), OpenACC (Open accelerators), Photoacoustic imaging, beamforming, Parallel computing, double-stage delay-multiply-and-sum (DS-DMAS), eigenspace-based minimum variance, linear-array imaging.

1. INTRODUCTION

Photoacoustic imaging (PAI) is a promising biomedical imaging modality which provides structural, molecular and functional information.[1,2] In this imaging modality, the tissue is irradiated by a laser pulse. Furthermore, photoacoustic waves are produced based on the thermoelastic expansion effects. In final stage, wide-band ultrasound transducers detect the radiated and propagated photoacoustic waves.[3,4] In comparison with the ultrasound imaging, PAI leads to a higher contrast because the contrast agents in PAI come from differences in optical absorption of the tissue, not differences in physical impedance. Additionally, PAI causes a better resolution in comparison with the optical imaging whereas the ultrasonic waves are scattered 10^{-3} times slower than the optical waves.[5]

PAI has multiple applications including tumor detection,[6] cancer detection and staging,[7] ocular imaging,[8]

Further author information: (Send correspondence to Mohsen Ghaffari-Miab)
Mohsen Ghaffari-Miab: E-mail: mghaffari@modares.ac.ir

Photons Plus Ultrasound: Imaging and Sensing 2019, edited by Alexander A. Oraevsky, Lihong V. Wang,
Proc. of SPIE Vol. 10878, 108785C · © 2019 SPIE · CCC code: 1605-7422/19/$18 · doi: 10.1117/12.2511115

molecular imaging,[9] functional imaging,[10,11] oncology,[12] ophthalmology[13] and cardiology.[14]

There are two kinds of PAI system; photoacoustic microscopy and photoacoustic tomography (PAT).[15] The main concentration of this paper is on the photoacoustic tomography. Ultrasound transducers in various types (circular, linear and arc) are being used to detect the photoacoustic waves. At the end, by mathematics, optical absorption map of the tissue is achieved.[16–18] Circular detection of the photoacoustic waves is hard to interpret into clinical applications.[19] To this end, linear-array ultrasound transducers are being utilized.[20] In linear-array PAT, image formation is one of the challenges. This is mainly because only a limited number of angles (about 40°) are available for signal detection, which leads to a low quality image (in comparison with the circular scenario). To address this issue, improved image formation algorithms should be utilized.[21–26]

Delay and sum (DAS) is mainly used for linear-array image formation scenario. However, it provides a low quality image because of its blindness. Actually, DAS is a popular algorithm due to its simple and easy implementation. Delay-multiply and sum (DMAS) was utilized to enhance the photoacoustic or ultrasound image quality, in comparison with DAS.[27,28]
As seen in the previous publications, researchers have enhanced image quality along with a higher processing complexity. Actually, the higher complexity of algorithms will reduce the temporal resolution and prevents real-time imaging.

Graphics Processing Unit (GPU) hardware along with the central processing unit (CPU) are being utilized to solve this problem. In comparison with the past, because of the hardware technology advantages, parallel processing power, and powerful parallelism directives,[29–31] GPU has been largely utilized in PAI systems.[32–39]
Recently, we have proposed double-stage delay-multiply-and-sum (DS-DMAS) leading to a higher contrast in comparison with DMAS.[22,23] We have also applied this algorithm for a LED-based PAI system.[40] In this paper, since the higher performance and efficiency of the DS-DMAS algorithm for linear-array PAT has been validated before, we enhance the temporal resolution of this algorithm by GPU implementation. It is shown that efficient GPU implementation of the DS-DMAS along with CPU decreases the execution time of DS-DMAS dramatically.

2. BACKGROUND

At first, DAS is introduced for photoacoustic image reconstruction. Later, DMAS is suggested to address the low performance of the DAS. The DMAS uses a correlation process to enhance the SNR which leads to higher image quality. However, the DMAS performance is reduced at the presence of high level of imaging noise. To solve this problem, DS-DMAS algorithm was recently introduced.[22,23]

2.1 GPU Implementation

In 2011, the open accelerators (OpenACC) programming model was introduced by NVIDIA company which allows programmers to accelerate the programs with no need to manipulate data communications between the host (CPU) and device (GPU). This level of programming is actually an open-directives routine that simplifies parallel programming. The OpenACC makes the GPU programming more straight and portable compared to a low-level model, like CUDA. In this paper, double precision OpenACC is used for implementing the DS-DMAS on GPU. The hardware used to implement and run the DS-DMAS are the Intel core-$i7$ 4790 CPU containing four physical cores and eight logical cores, NVIDIA GTX 760 with 1152 CUDA cores, and GPU NVIDIA GTX 1070 having 1920 CUDA cores. To make the comparison of processing time fair, the utilized CPU and GPU are opted at the nearly similar price range.

2.1.1 OpenACC Implementation

The OpenACC programming model, suggested by NVIDIA, CAPS, Cray, and Portland Group, is a user-driven directive-based general parallel programming model designed for scientists and engineers. In OpenACC, the programmer is able to insert library routines and compiler directives to Fortran, C, or C++ source code to assign the area in the code that should be accelerated in parallel on GPU. In fact, the programmer is not preoccupied with parallelism details leaving these routines to the compiler. This programming model efficiently and intelligently launches the kernels on GPU.[41]

In the OpenACC execution, each GPU thread computes the brightness value of an exact pixel assigned by the programmer. In GPU, threads are arranged in a three-level hierarchy. Each block contains threads, and the thread blocks are grouped into grids. The OpenACC performance model has three stages: 1) Gang (Thread

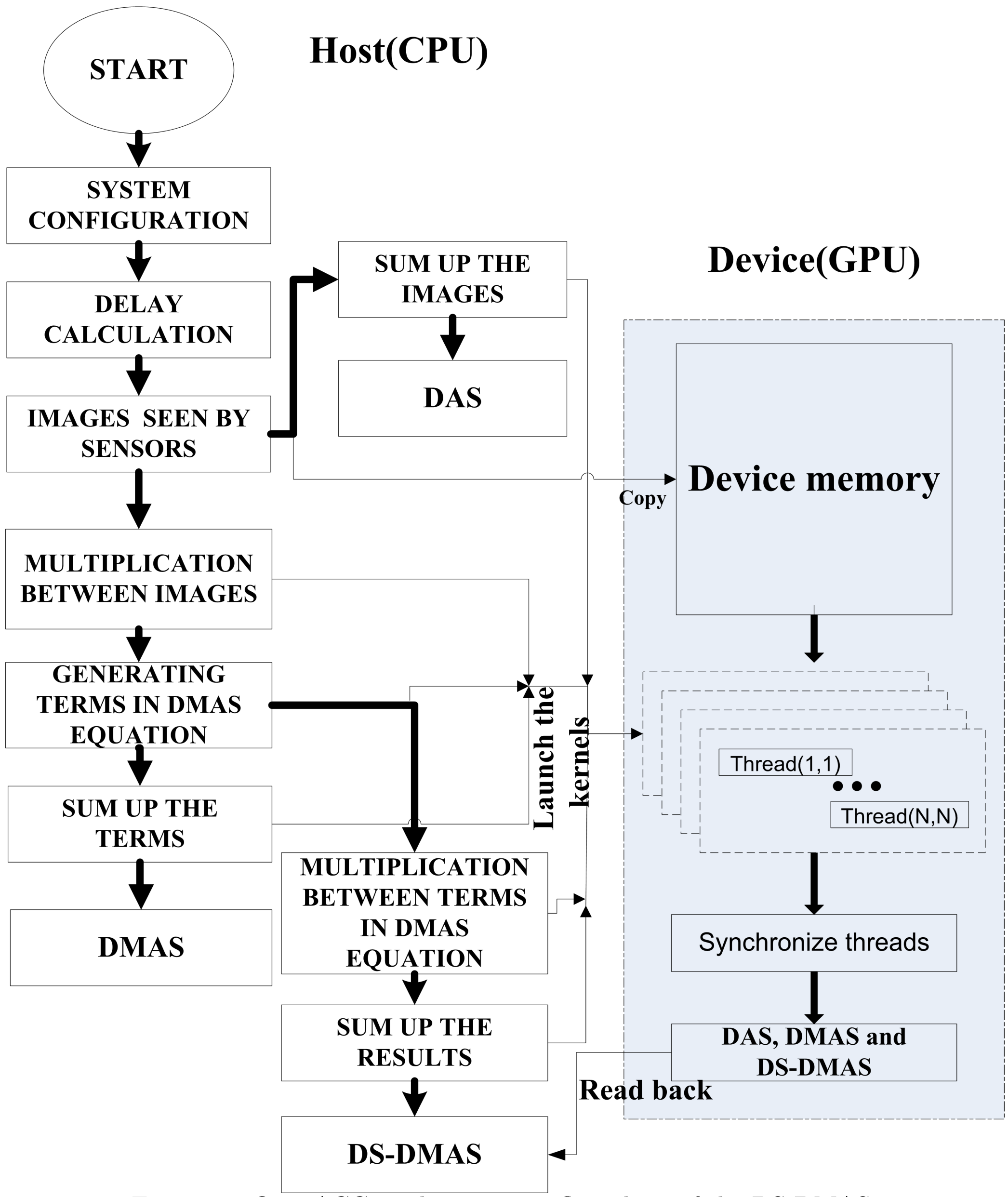

Figure 1: OpenACC implementation flow chart of the DS-DMAS.

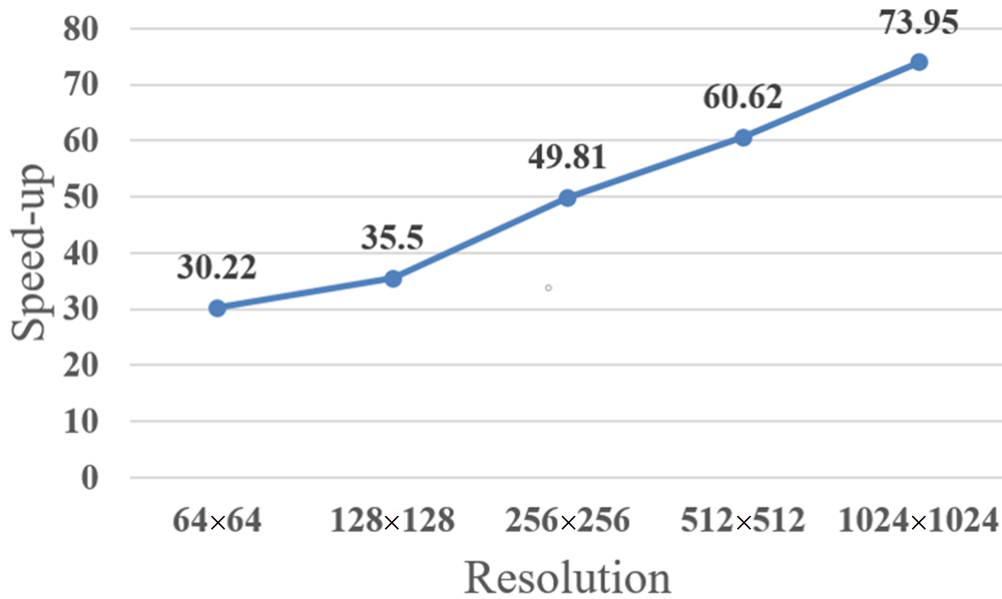

Figure 2: OpenACC speed-up for various number of image pixels.

Table 1: Performance comparison of the optimized OpenACC DS-DMAS implementation. The size of image is 1024×1024.

Implementation	processing Time(s)	Speed-up
CPU MATLAB	665.53	1
CPU FORTRAN serial	570.8	1.166
Optimized OpenACC NVIDIA 760 GPU	18	36.97
Optimized OpenACC NVIDIA 1070 GPU	9	73.95

block), 2)Worker (Warp), and, 3)Vector (Threads in a Warp). The gangs, vectors, and workers can automatically be configured by OpenACC compiler directives in an optimum approach, with least data transfers between CPU and GPU hardware. The code annotated with OpenACC routines can result in a considerable speed-up in execution time compared to the serial code on CPU.

As shown in Fig .1, the OpenACC implementation of the DS-DMAS algorithm includes the following five steps:

- Allocating memory on GPU (OpenACC compiler doing that job automatically).
- Transferring the needed data from CPU to GPU, for just one time using OpenACC Data Clause.
- Launching GPU Kernels for execution (OpenACC compiler efficiently and intelligently launches the kernels and parallels the code on GPU).
- Transferring result (final reconstructed image by DS-DMAS algorithm) from GPU to CPU with using OpenACC Data Clause.

2.1.2 Speed-up evaluation

As given in Table 1, the speed-up for a photoacoustic image having 1024×1024 pixels is assessed for optimized OpenACC on the NVIDIA GTX 760 GPU and NVIDIA GTX 1070 GPU. It is worth to mention that the efficient MATLAB code is utilized for comparison. Actually, the memory access is optimized using matrix operations instead of using nested loops. The attained speed-up by executing optimized OpenACC fortran code is almost 73.95 times compared to the optimized and efficient MATLAB code, without losing accuracy. Fig .2 shows the OpenACC speed-up versus various number of image pixels. As seen, the assessed speed-up ratio is increased

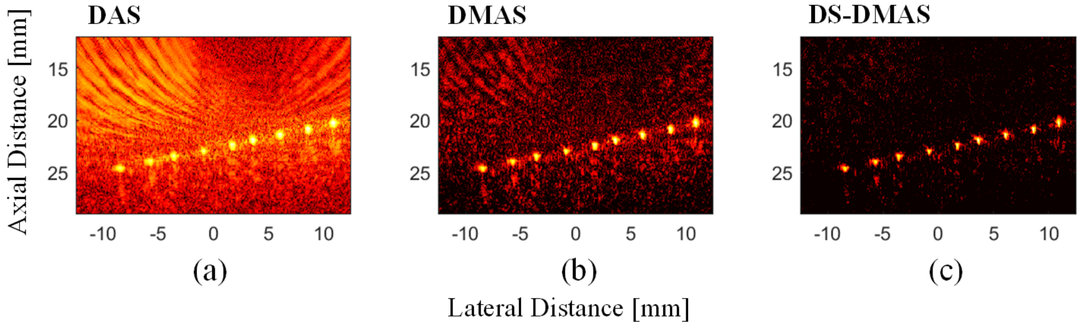

Figure 3: Reconstructed photoacoustic images using (a) DAS, (b) DMAS and (c) DS-DMAS. All the images are shown with a dynamic range of 60 dB.

by increasing the number of the image pixels while the precision of the algorithm is preserved. The relative error for computed pixels value in double precision OpenACC programming model compared with the sequential implementation on CPU is in the order of 10^{-13}.

2.2 DS-DMAS evaluation

DS-DMAS algorithm provides higher performance has been widely assessed in previous publications.[22,23] We have presented the output images after processing to briefly review the improvement achieved by the DS-DMAS. Also, it is noteworthy that the reconstruction process is executed on GPU and CPU. However, the major computation part of the reconstruction image is executed on the GPU. The output images after processing are shown in Fig. 3. DAS algorithm generates images with high sidelobe level. Furthermore, the background noise affects the output image. As seen in Fig. 3(a) and Fig. 3(b), DMAS provides a higher noise suppression and enhances the image quality, in comparison with the DAS. As shown in Fig. 3(c), DS-DMAS performs better than other algorithms in terms of sidelobes reduction and noise suppression. Quantitatively, The DS-DMAS leads to about 39 dB and 20 dB sidelobes reduction, in comparison with DAS and DMAS algorithms, respectively.

3. CONCLUSION

In this paper, the DS-DMAS is implemented in parallel on GPU. This algorithm was used for photoacoustic image reconstruction. The OpenACC code was optimized in three levels. At the final stage, it was shown that the OpenACC implementation on GPU has gained a speed-up of nearly 74×, compared to the sequential implementation on CPU, for an image containing 1024×1024 pixels. Moreover, it was shown that with increasing the number of pixels of the photoacoustic image, a higher speed-up is achieved. The proposed GPU implementation provides the possibility to have photoacoustic images reconstructed in a size of 128×128, and 256×256 with a frame rate of 3 and 2, respectively.

REFERENCES

[1] Wang, X., Xie, X., Ku, G., Wang, L. V., and Stoica, G., "Noninvasive imaging of hemoglobin concentration and oxygenation in the rat brain using high-resolution photoacoustic tomography," *Journal of biomedical optics* **11**(2), 024015 (2006).

[2] Wang, J., Lin, C.-Y., Moore, C., Jhunjhunwala, A., and Jokerst, J. V., "Switchable photoacoustic intensity of methylene blue via sodium dodecyl sulfate micellization," *Langmuir* **34**(1), 359–365 (2017).

[3] Jokerst, J. V., Thangaraj, M., Kempen, P. J., Sinclair, R., and Gambhir, S. S., "Photoacoustic imaging of mesenchymal stem cells in living mice via silica-coated gold nanorods," *ACS nano* **6**(7), 5920–5930 (2012).

[4] Kim, T., Lemaster, J. E., Chen, F., Li, J., and Jokerst, J. V., "Photoacoustic imaging of human mesenchymal stem cells labeled with prussian blue–poly (l-lysine) nanocomplexes," *ACS nano* **11**(9), 9022–9032 (2017).

[5] Wang, L. V. and Hu, S., "Photoacoustic tomography: in vivo imaging from organelles to organs," *Science* **335**(6075), 1458–1462 (2012).

[6] Pramanik, M., Ku, G., Li, C., and Wang, L. V., "Design and evaluation of a novel breast cancer detection system combining both thermoacoustic (ta) and photoacoustic (pa) tomography," *Medical physics* **35**(6Part1), 2218–2223 (2008).

[7] Mehrmohammadi, M., Joon Yoon, S., Yeager, D., and Y Emelianov, S., "Photoacoustic imaging for cancer detection and staging," *Current molecular imaging* **2**(1), 89–105 (2013).

[8] Hariri, A., Wang, J., Kim, Y., Jhunjhunwala, A., Chao, D. L., and Jokerst, J. V., "In vivo photoacoustic imaging of chorioretinal oxygen gradients," *Journal of biomedical optics* **23**(3), 036005 (2018).

[9] Pu, K., Shuhendler, A. J., Jokerst, J. V., Mei, J., Gambhir, S. S., Bao, Z., and Rao, J., "Semiconducting polymer nanoparticles as photoacoustic molecular imaging probes in living mice," *Nature nanotechnology* **9**(3), 233 (2014).

[10] Yao, J., Xia, J., Maslov, K. I., Nasiriavanaki, M., Tsytsarev, V., Demchenko, A. V., and Wang, L. V., "Noninvasive photoacoustic computed tomography of mouse brain metabolism in vivo," *Neuroimage* **64**, 257–266 (2013).

[11] Nasiriavanaki, M., Xia, J., Wan, H., Bauer, A. Q., Culver, J. P., and Wang, L. V., "High-resolution photoacoustic tomography of resting-state functional connectivity in the mouse brain," *Proceedings of the National Academy of Sciences* **111**(1), 21–26 (2014).

[12] Valluru, K. S., Wilson, K. E., and Willmann, J. K., "Photoacoustic imaging in oncology: translational preclinical and early clinical experience," *Radiology* **280**(2), 332–349 (2016).

[13] Song, W., Wei, Q., Liu, W., Liu, T., Yi, J., Sheibani, N., Fawzi, A. A., Linsenmeier, R. A., Jiao, S., and Zhang, H. F., "A combined method to quantify the retinal metabolic rate of oxygen using photoacoustic ophthalmoscopy and optical coherence tomography," *Scientific reports* **4**, 6525 (2014).

[14] Taruttis, A., Herzog, E., Razansky, D., and Ntziachristos, V., "Real-time imaging of cardiovascular dynamics and circulating gold nanorods with multispectral optoacoustic tomography," *Optics express* **18**(19), 19592–19602 (2010).

[15] Wang, L. V., "Multiscale photoacoustic microscopy and computed tomography," *Nature photonics* **3**(9), 503 (2009).

[16] Mozaffarzadeh, M., Yan, Y., Mehrmohammadi, M., and Makkiabadi, B., "Enhanced linear-array photoacoustic beamforming using modified coherence factor," *Journal of biomedical optics* **23**(2), 026005 (2018).

[17] Xu, M., Xu, Y., and Wang, L. V., "Time-domain reconstruction algorithms and numerical simulations for thermoacoustic tomography in various geometries," *IEEE Transactions on biomedical engineering* **50**(9), 1086–1099 (2003).

[18] Mozaffarzadeh, M., Periyasamy, V., Pramanik, M., and Makkiabadi, B., "Efficient nonlinear beamformer based on pth root of detected signals for linear-array photoacoustic tomography: application to sentinel lymph node imaging," *Journal of Biomedical Optics* **23**(12), 121604 (2018).

[19] Upputuri, P. K. and Pramanik, M., "Recent advances toward preclinical and clinical translation of photoacoustic tomography: a review," *Journal of Biomedical Optics* **22**(4), 041006 (2016).

[20] Sivasubramanian, K., Periyasamy, V., Dienzo, R. A., and Pramanik, M., "Hand-held, clinical dual mode ultrasound-photoacoustic imaging of rat urinary bladder and its applications," *Journal of biophotonics* **11**(5), e201700317 (2018).

[21] Mozaffarzadeh, M., Mahloojifar, A., Orooji, M., Kratkiewicz, K., Adabi, S., and Nasiriavanaki, M., "Linear-array photoacoustic imaging using minimum variance-based delay multiply and sum adaptive beamforming algorithm," *Journal of biomedical optics* **23**(2), 026002 (2018).

[22] Mozaffarzadeh, M., Sadeghi, M., Mahloojifar, A., and Orooji, M., "Double-stage delay multiply and sum beamforming algorithm applied to ultrasound medical imaging," *Ultrasound in Medicine and Biology* **44**(3), 677 – 686 (2018).

[23] Mozaffarzadeh, M., Mahloojifar, A., Orooji, M., Adabi, S., and Nasiriavanaki, M., "Double-stage delay multiply and sum beamforming algorithm: Application to linear-array photoacoustic imaging," *IEEE Transactions on Biomedical Engineering* **65**(1), 31–42 (2018).

[24] Park, S., Karpiouk, A. B., Aglyamov, S. R., and Emelianov, S. Y., "Adaptive beamforming for photoacoustic imaging using linear array transducer," in [*Ultrasonics Symposium, 2008. IUS 2008. IEEE*], 1088–1091, IEEE (2008).

[25] Paridar, R., Mozaffarzadeh, M., Mehrmohammadi, M., and Orooji, M., "Photoacoustic image formation based on sparse regularization of minimum variance beamformer," *Biomedical Optics Express* **9**(6), 2544–2561 (2018).

[26] Paridar, R., Mozaffarzadeh, M., Periyasamy, V., Basij, M., Mehrmodammadi, M., Pramanik, M., and Orooji, M., "Validation of delay-multiply-and-standard-deviation weighting factor for improved photoacoustic imaging of sentinel lymph node," *Journal of biophotonics* , e201800292 (2018).

[27] Alshaya, A., Harput, S., Moubark, A. M., Cowell, D. M., McLaughlan, J., and Freear, S., "Spatial resolution and contrast enhancement in photoacoustic imaging with filter delay multiply and sum beamforming technique," in [*Ultrasonics Symposium (IUS), 2016 IEEE International*], 1–4, IEEE (2016).

[28] Matrone, G., Savoia, A. S., Caliano, G., and Magenes, G., "The delay multiply and sum beamforming algorithm in ultrasound b-mode medical imaging," *IEEE Transactions on Medical Imaging* **34**(4), 940–949 (2015).

[29] Mokdad, A., Azmi, P., Mokari, N., Moltafet, M., and Ghaffari-Miab, M., "Cross-layer energy efficient resource allocation in pd-noma based h-crans: Implementation via gpu," *IEEE Transactions on Mobile Computing* , 1–1 (2018).

[30] Masumnia-Bisheh, K., Ghaffari-Miab, M., and Zakeri, B., "Evaluation of different approximations for correlation coefficients in stochastic fdtd to estimate sar variance in a human head model," *IEEE Transactions on Electromagnetic Compatibility* **59**, 509–517 (April 2017).

[31] Pratx, G. and Xing, L., "Gpu computing in medical physics: A review," *Medical physics* **38**(5), 2685–2697 (2011).

[32] Kang, H., Lee, S.-W., Lee, E.-S., Kim, S.-H., and Lee, T. G., "Real-time gpu-accelerated processing and volumetric display for wide-field laser-scanning optical-resolution photoacoustic microscopy," *Biomedical optics express* **6**(12), 4650–4660 (2015).

[33] Shan, T., Qi, J., Jiang, M., and Jiang, H., "Gpu-based acceleration and mesh optimization of finite-element-method-based quantitative photoacoustic tomography: a step towards clinical applications," *Applied optics* **56**(15), 4426–4432 (2017).

[34] Ding, L., Deán-Ben, X. L., and Razansky, D., "Real-time model-based inversion in cross-sectional optoacoustic tomography," *IEEE transactions on medical imaging* **35**(8), 1883–1891 (2016).

[35] Shan, T., "Accelerated time domain quantitative photoacoustic tomography (td-qpat) based on graphic processing units (gpu) for clinical application of breast cancer imaging," in [*Optical Tomography and Spectroscopy*], OW4D–3, Optical Society of America (2018).

[36] Liu, S., Feng, X., Gao, F., Jin, H., Zhang, R., Luo, Y., and Zheng, Y., "Gpu-accelerated two dimensional synthetic aperture focusing for photoacoustic microscopy," *APL Photonics* **3**(2), 026101 (2018).

[37] Wang, K., Huang, C., Kao, Y.-J., Chou, C.-Y., Oraevsky, A. A., and Anastasio, M. A., "Accelerating image reconstruction in three-dimensional optoacoustic tomography on graphics processing units," *Medical physics* **40**(2) (2013).

[38] Lutzweiler, C., Deán-Ben, X. L., and Razansky, D., "Expediting model-based optoacoustic reconstructions with tomographic symmetries," *Medical physics* **41**(1) (2014).

[39] Arridge, S., Beard, P., Betcke, M., Cox, B., Huynh, N., Lucka, F., Ogunlade, O., and Zhang, E., "Accelerated high-resolution photoacoustic tomography via compressed sensing," *Physics in Medicine & Biology* **61**(24), 8908 (2016).

[40] Mozaffarzadeh, M., Hariri, A., Moore, C., and Jokerst, J. V., "The double-stage delay-multiply-and-sum image reconstruction method improves imaging quality in a led-based photoacoustic array scanner," *Photoacoustics* **12**, 22 – 29 (2018).

[41] Rostami, S. R. M. and Ghaffari-Miab, M., "Fast computation of finite difference generated time-domain green's functions of layered media using openacc on graphics processors," in [*2017 Iranian Conference on Electrical Engineering (ICEE)*], 1596–1599 (May 2017).